Journal of Environmental Chemical Engineering 9 (2021) 105827

Contents lists available at ScienceDirect

Journal of Environmental Chemical Engineering

journal homepage: www.elsevier.com/locate/jece

The photocatalytic degradation of sodium diclofenac in different water matrices using g-C_3N_4 nanosheets: A study of the intermediate by-products and mechanism

Marta Jiménez-Salcedo [a], Miguel Monge [a,b], María Teresa Tena [a,*]

[a] Department of Chemistry, University of La Rioja, C/Madre de Dios 53, E-26006 Logroño, La Rioja, Spain
[b] Centro de Investigación en Síntesis Química (CISQ). University of La Rioja, C/ Madre de Dios 53, E-26006 Logroño, La Rioja, Spain

ARTICLE INFO

Editor: Dr. G. Palmisano

Keywords:
Diclofenac
g-C_3N_4
Photocatalysis
By-products
High resolution mass spectrometry
Tap water

ABSTRACT

The photocatalytic degradation of sodium diclofenac (a nonsteroidal anti-inflammatory drug) in both ultrapure water and tap water with nanosheets of graphitic carbon nitride (g-C_3N_4) as catalyst and utilising two different sources of visible light (low-power (4 × 10 W) white light LEDs and natural sunlight) was carried out and compared. The highest depletion rate was observed for the system with tap water and natural sunlight. All photodegradations followed pseudo-first-order kinetics. A degradation pathway for sodium diclofenac has been proposed and four photodegraded products formed along with the diclofenac depletion have been detected by liquid chromatography coupled with high-resolution mass spectrometry using a QToF instrument. The accurate mass obtained for the detected ions together with the MS/MS data allowed us to propose chemical structures for the by-products. Moreover, a study to identify the main active species involved in the degradation mechanism was undertaken by introducing scavengers to quench the photodegradations: a N_2 atmosphere for superoxide radicals ($\cdot O_2^-$), triethanolamine for photoexcited holes (h^+) and tert-butanol for hydroxyl radicals ($\cdot OH$).

1. Introduction

In the last few decades, water quality is an issue which has gathered a lot of attention. Myriad pharmaceuticals have been found in diverse aquatic environments (surface waters, groundwater, and/ or tap water) [1] in several countries. Drugs cannot be completely removed by Wastewater Treatment Plants (WWTPs). Remediation efficiency might be less than 10% in the case of drugs such as diclofenac (DCF) because WWTPs are commonly designed to handle organic matter in the mg/L range [2] yet. DCF has been detected at a lower range (μg/L) in both treated water and surface water [3]. DCF is a nonsteroidal anti-inflammatory drug (NSAID), in wide usage on a global scale. It is particularly dangerous because as a chlorinated micropollutant it presents characteristics such as: low biodegradability, high toxicity, long-term persistence in the environment and strong bio-accumulative potential [4]. For this reason, advanced photocatalytic oxidation technologies have been the subject of thorough research.

For the photodegradation of DCF in water, different catalytic processes have been studied: photolysis [5–7], sonolysis [8], sonophotolysis [8], sonophotocatalysis [9] and photocatalysis. A large number of catalysts have been used for the photocatalysis process, such as: TiO_2 [8, 10], Ag/TiO_2 [9], ZnO, Fe-ZnO [8], TiO_2/BiOI [11], Pd/Al_2O_3 [4], g-C_3N_4 [12–14] or g-C_3N_4 hybrid composites such as: Co_3O_4/g-C_3N_4 [14], TiO_2/g-C_3N_4 [15], Ti_3C_2/g-C_3N_4 [16], V_2O_5/boron doped g-C_3N_4 [13], Ag/g-C_3N_4 [17], AgI/g-C_3N_4 [18], Ag_3PO_4/g-C_3N_4 [19].

The well-known semiconductor TiO_2, which has a wide band gap, has commonly been used in photocatalysis, however the fact that this type of semiconductor cannot absorb visible light (it can only absorb UV light due to its band gap) is a major disadvantage for practical applications, especially considering that UV light only represent 4% of total solar radiation. A semiconductor with a narrower band gap, such as graphitic carbon nitride (g-C_3N_4), which is able to take advantage of the visible light of the solar spectrum (approximately 43%), has been postulated as a material of interest for many reasons: (i) its low band gap, which makes it a suitable material for visible light applications, (ii) it is a stable compound and (iii) the abundance of precursors (dicyanamide, melamine, urea, cyanamide, thiourea or ammonium thiocyanate) for facile synthesis [20], to name just a few.

In the present study, the photocatalytic behaviours of natural sunlight and low power LED lamps were evaluated for the degradation of

* Corresponding author.
E-mail addresses: marta.jimenez@unirioja.es (M. Jiménez-Salcedo), miguel.monge@unirioja.es (M. Monge), maria-teresa.tena@unirioja.es (M.T. Tena).

https://doi.org/10.1016/j.jece.2021.105827
Received 16 April 2021; Received in revised form 19 May 2021; Accepted 6 June 2021
Available online 8 June 2021

DCF in tap water and ultrapure water using g-C_3N_4 nanosheets as catalyst. The effect of two water matrices was compared with two sources of irradiation, which is unique to this study. The low power LEDs make it possible to study the kinetics of intermediates and the degradation mechanism. This type of comparative study might be helpful for the future implementation of this technology in real-life applications. Furthermore, the intermediates formed in the degradation were identified by high-resolution mass spectrometry. This technique made it possible to calculate the elementary composition of the by-products and to propose identifications. This technique yielded promising results in prior studies involving ibuprofen and ciprofloxacin [21,22]. In view of the results of the main active species responsible for the photodegradations, a plausible degradation mechanism has also been proposed.

2. Experimental

2.1. Chemical reagents

Sodium diclofenac (DCF) ($\geq$ 99%), tert-butanol and triethanolamine were provided by Sigma-Aldrich (Germany). HPLC-grade acetonitrile came from Scharlab (Barcelona, Spain). Formic acid (98%) for mass spectrometry was purchased from Fluka Analytical. Melamine (99%) was obtained from Alfa Aesar (Germany). All chemicals were used as received without further purification.

2.2. Synthesis and characterisation of g-C_3N_4 catalyst

The graphitic carbon nitride photocatalyst was synthesised by heating melamine in a crucible, in order to prevent sublimation in air as former authors reported [22,23]. In a typical synthesis, 5 g of melamine were heated in an oven in two stages: 500 °C for 4 h, followed by a second round at 520 °C for 2 h in order to produce thermal oxidative exfoliation of the material.

The light absorbance properties and morphology of the light yellowish material employed as a catalyst were characterised by transmission electron microscopy (TEM), solid UV–Vis diffuse reflectance spectroscopy and X-ray photoelectron spectroscopy (XPS). The stability of the catalyst was assessed by Fourier-transform infra-red spectroscopy (FTIR).

2.3. Photodegradation procedure and detection of active species

In a typical DCF photodegradation, 45.5 mg of g-C_3N_4 were suspended in 70 mL of a 3 μg/mL DCF aqueous solution (ultrapure water or tap water depending on the experiment; the tap water quality parameters are listed in Table S1). The reactions were performed in a Schlenk glass reactor (Fig. S1). The suspension was sonicated for 2 min in order to disperse the photocatalyst properly. After that, it was stirred for 40 min in dark conditions to establish the adsorption/desorption equilibrium before the photocatalytic reaction. Then, the mixture was irradiated with two different sources of light, depending on the experiment. The experiments performed with natural sunlight were carried out outdoors, with an average temperature of 30 °C and an ultraviolet index of 6–9, accordingly to the Spanish National Agency of Meteorology (www.AMET.es). The specific meteorological data for each experiment is collected in Supplementary material Table S2. The assembly employed in visible LED light experiments consists of four 10 W white light LED lamps (LED-Engin, CA, USA) placed equidistantly inside a cylinder with cooling water circulating inside it to maintain the glass reactor at a constant temperature of 25 °C. The experimental setups for natural sunlight and visible light radiation are shown in Fig. S1 of the Supplementary material. In order to study the effect of active species on the photodegradation reaction, the corresponding scavengers were introduced into the solution to quench the specific reactive species, in ultrapure water irradiated with visible light. The reactions were monitored under three different conditions: in a 10^{-3} M aqueous solution of tert-butanol for ·OH (hydroxyl radicals) scavenging, in a 10^{-3} M aqueous solution of triethanolamine for h^+ (photogenerated holes) scavenging and by bubbling inert N_2 gas to avoid O_2 in the solution for $\cdot O_2^-$ (superoxide radicals) scavenging.

During the irradiation period, the aqueous solution was vigorously stirred, and aliquots were withdrawn at different times to monitor the reaction. All samples were filtered with PTFE hydrophilic filters (13 mm, 0.22 μm) before the chromatographic analysis and stored at 4 °C until further analysis.

For the DCF by-products identification, the degradation was performed with natural sunlight and 90 mg of the catalyst were suspended in 70 mL of a 90 μg/mL tap water solution of DCF.

2.4. Analytical procedures

The DCF intermediate by-products were analysed using a LC-MS/MS instrument previously described [21], a C18 column and a mobile phase gradient programme consisting of an aqueous solution and acetonitrile, both containing 0.1% (v/v) formic acid. The mass spectra data were obtained in both positive and negative mode. Further parameters are summarised in Supplementary material (Text S1).

Samples for routine DCF analysis, such as monitoring by-product formation during photocatalytic experiments or calculating the kinetics constants, were analysed by HPLC-UV and detection wavelength was 276 nm. The column used in the separation was a C18 and the isocratic mobile phase consisted of 60:40 aqueous solution/acetonitrile, both containing 0.1(v/v) formic acid. (Further information about the equipment in Supplementary material, Text S2). As previously stated, all samples were filtered before the chromatographic analysis.

The toxicology assessment of the DCF degraded products was evaluated employing Toxtree v3.1.0.1851 software, utilising the Cramer classification scheme.

3. Results and discussion

3.1. Characterisation and stability of the 2D g-C_3N_4 photocatalyst

The catalyst g-C_3N_4 was characterised in previous studies [21,22] by transmission electronic microscopy (TEM) and UV–vis diffuse reflectance. Additionally, XPS analyses of g-C_3N_4 provide relevant information about the elemental composition at the surface of the material. Fig. 1 shows representative TEM images and the Tauc plot of 2D-nanosheets of g-C_3N_4 of ca. 50–100 nm with 2.79 eV of semiconductor band gap. Other authors have reported slightly different values for the g-C_3N_4 band gap: 2.8 eV for bulk g-C_3N_4 and 2.94 eV for exfoliated g-C_3N_4 [24]. The band edge positions of the conduction band (CB) and the valence band (VB) for g-C_3N_4 may be estimated [25]. Thus, at the point of zero charge, the VB edge (E_{VB}) and the CB edge (E_{CB}) of a semiconductor can be calculated using the equations:

$$E_{VB} = X - E_e + 0.5E_g$$

$$E_{CB} = E_{VB} - E_g$$

where X is the absolute electronegativity of a given semiconductor (geometric mean of the absolute electronegativity of the atoms forming the semiconductor); E_e is the energy of the free electrons (ca. 4.5 eV); E_g is the band gap energy of the semiconductor. The absolute electronegativity (X) for g-C_3N_4 is 4.73, which leads to a valence band edge (E_{VB}) of 1.63 eV and to a conduction band edge (E_{CB}) of −1.17 eV for our obtained band gap energy of 2.79 eV. These values enable the construction of a schematic diagram of the photoexcited electron-hole separation process for the explanation of the reaction mechanisms of the g-C_3N_4 photocatalyst and the determination of the reactive oxygen species (*vide infra*).

The wide XPS spectrum of g-C_3N_4 displays the presence of intense

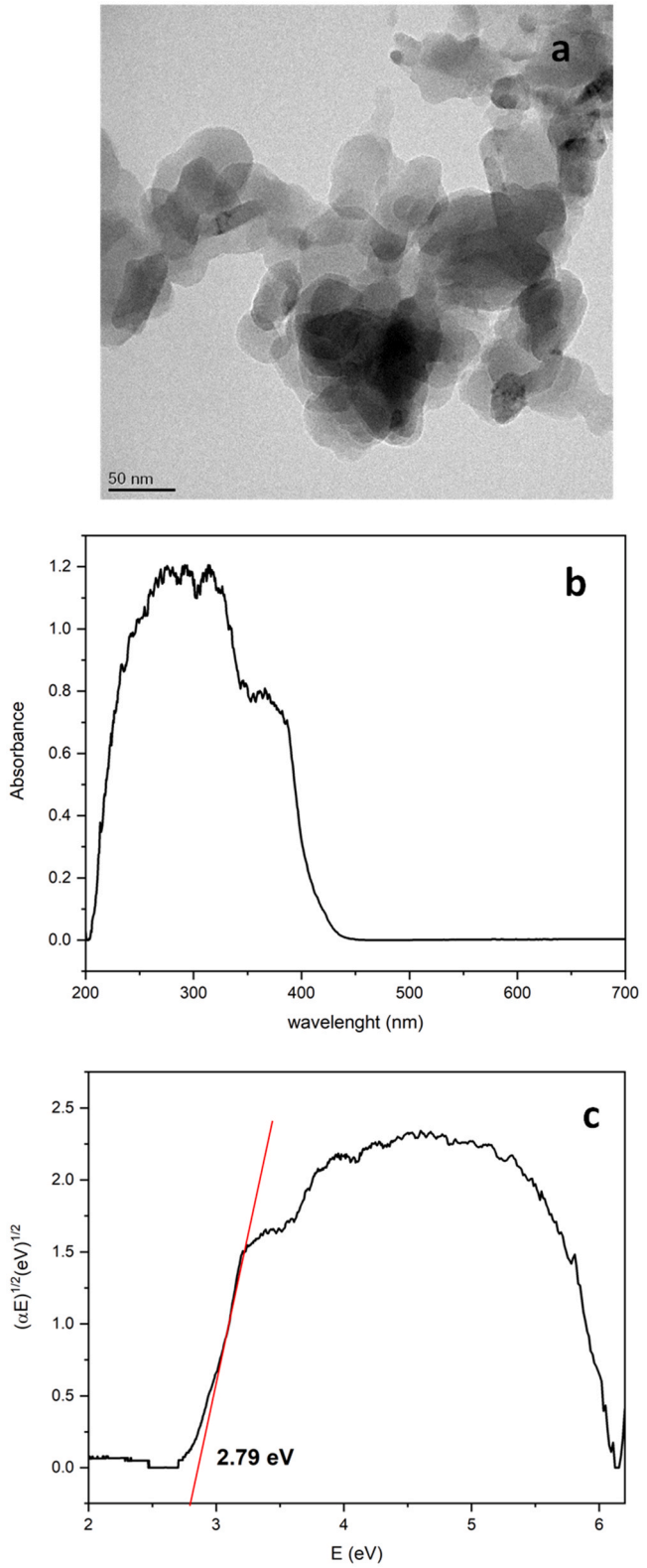

Fig. 1. Representative TEM image of the corresponding g-C_3N_4 (a). Diffuse reflectance UV–Vis spectrum of solid g-C_3N_4 (b). Tauc plot for g-C_3N_4 (c).

peaks corresponding to C and N (see Fig. S2a in Supplementary material). From the analysis of this wide spectrum, it can be observed that the atomic composition % of C and N atoms is 39.9% and 58.8%, respectively, pointing to a C:N ratio of 0.68, slightly below the theoretical one of 0.75.

Fig. S2c depicts the high-resolution XPS spectrum for the C 1s region for g-C_3N_4, which is fitted into four peaks. The intense peak at 288.4 eV is assigned to the sp^2 carbon atoms in the triazine units of g-C_3N_4 (C—N═C). This observation is supported by the presence of the weak peak component of the C 1s region at 293.7, which is attributed to double bond π-excitations. The peak at 288.9 eV would be related to C—O bonds, while the peak at 285.1 is associated with C—C bonds. Fig. S2d displays the high-resolution spectrum of the N 1s region, which is also fitted into four peaks. The intense peak at 398.5 eV is associated with sp^2 N atoms in the triazine unit (C—N═C), which is also related to the weak peak at 404.1 eV due to the double bond π-excitations. The weak peak at 399.2 eV is related to the N atoms between aromatic rings in the g-C_3N_4 structure, whereas the presence of NH_2 groups is assigned to the peak at 400.8 eV [26,27]. The high-resolution XPS spectrum for the O 1s region (Fig. S2b) shows a weak peak at 532.3 eV attributed to adsorbed water molecules (532.6 eV).

The stability of the catalyst was an important factor for its practical application. No obvious changes in the IR spectrum (Fig. S3) of the fresh and used g-C_3N_4 were observed, supporting the high-stability of the material. The only important difference is the presence of a broad absorption at ca. 3500 cm^{-1} in the IR spectrum of g-C_3N_4 after photocatalysis, arising from adsorbed water. The rest of the common absorptions usually assigned to g-C_3N_4 at ca. 820 cm^{-1} (breathing mode of triazine units) and in the 1100–1700 cm^{-1} range (strong absorptions assigned to stretching modes of the CN heterocycles) remained unaltered.

3.2. Photocatalytic activity and detection of active species

To monitor the DCF degradation, samples at different intervals of time were analysed by HPLC-UV during the reaction. Fig. 2 shows the evolution of the DCF signal in both ultrapure water and tap water irradiated with natural sunlight and visible light, with and without catalyst, during the first 40 min of adsorption and during the irradiation period. Around 5% of DCF was adsorbed on the g-C_3N_4, regardless of the water matrix used in the experiment. As can be seen in Fig. 2, the degradation of diclofenac was negligible in the absence of a photocatalyst when the samples were irradiated with low power visible light. However, when employing a more powerful source of irradiation like natural sunlight, it was depleted after 150 min of light exposure. Some authors did not notice degradation of diclofenac in the absence of a catalyst with a visible light simulator [28], which implies that the photodegradability of diclofenac depends on the source of irradiation. The degradation rates observed in experiments with tap water were higher than those achieved in ultrapure water, which might be ascribed to the presence of chloride ions of salts, accordingly to the literature [3,4]. Moreover, the depletion of DCF in the experiments performed with natural sunlight was faster than in the visible light irradiated experiments, which agrees with nature of the two sources of light employed. The sunlight radiation is a high energetic combination of near infrarred, visible and ultraviolet light and the experiments were carried out in sunny days with high ultraviolet index. On the other hand, the LED light source consists of low power visible light emitters and the higher the power of the light, the faster the depletion of drugs, as some authors reported [29].

In tap water, the photocatalytic degradation of DCF followed the pseudo-first-order kinetics with apparent reaction rate constants 0.031 min^{-1} and 0.383 min^{-1} for low power visible light and natural sunlight, respectively. Whereas in ultrapure water the pseudo-first-order kinetic constants were 0.015 min^{-1} and 0.131 min^{-1} for low power visible light and natural sunlight, respectively (Fig. S4).

Other authors have reported similar constant values for DCF degradation with g-C_3N_4 (0.013 and 0.0141 min^{-1}) under high power visible light irradiation (300 W Xenon light) and those values raised to 0.561 and 0.0429 min^{-1} with g-C_3N_4/AgI and g-C_3N_4/Ag composites [17,18]. Whereas with similar visible light irradiation power, 0.0061 and

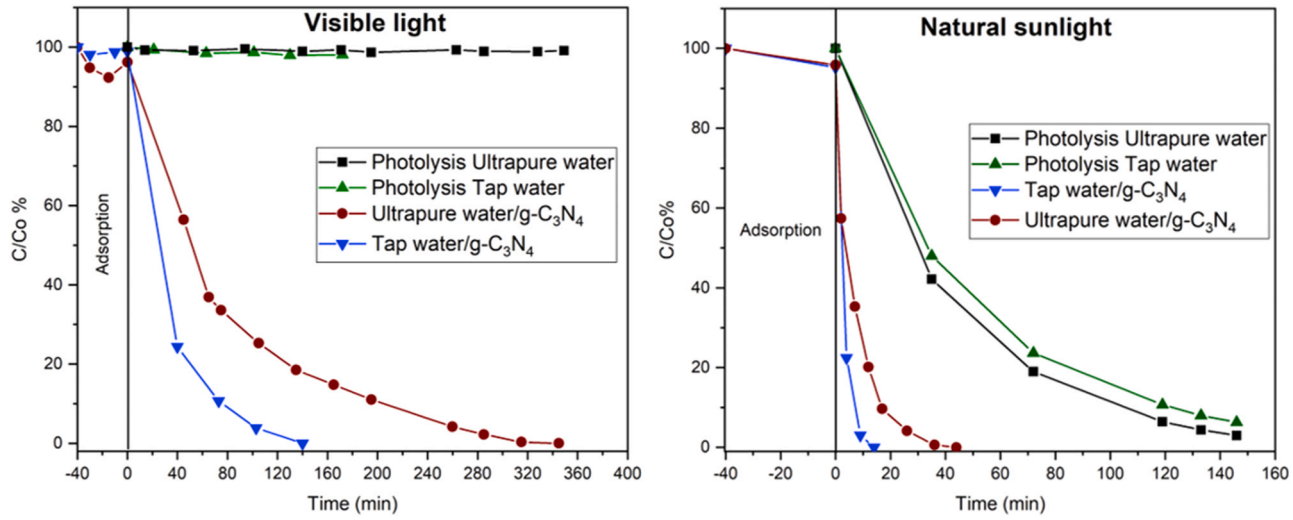

Fig. 2. Photocatalytic degradation of DCF with g-C_3N_4 under visible light and natural sunlight radiation in ultrapure water and tap water.

0.1796 min^{-1} apparent constants have been reported for g-C_3N_4 and g-C_3N_4/TiO_2 catalysts, respectively [15].

The light irradiation promotes electrons from the valence band (VB) to the conduction band (CB) of the n-type semiconductor, generating holes (h^+) in the VB and electrons (e^-) in the CB.

$$g\text{-}C_3N_4 + h\nu \rightarrow g\text{-}C_3N_4\ (e^-) + g\text{-}C_3N_4\ (h^+)$$

As it has been shown previously, the main reactive species for photocatalytic degradation are photogenerated holes (h^+), superoxide radicals ($\cdot O_2^-$), and hydroxyl radicals (·OH). To fully understand which of these species plays the major role in the photodegradation of DCF with g-C_3N_4, tert-butanol and triethanolamine were used as ·OH and h^+ scavengers, respectively. Also, the reaction was carried out after N_2 bubbling to remove O_2, thus avoiding the formation of superoxide radicals $\cdot O_2^-$ from photoexcited electrons [30–33].

Fig. 3 shows the influence of three scavengers on the depletion of DCF. The regression data for the kinetics are summarised in the Supplementary material (Fig. S4 and Table S3).

As shown in Fig. 3, the N_2 bubbling massively decreased the depletion of DCF and the photodegradation was almost completely quenched, suggesting that superoxide radicals ($\cdot O_2^-$) play the major role in the photocatalytic process. The addition of triethanolamine also decreases the depletion of DCF to some extent, which suggests that photogenerated holes (h^+) play an important role in the degradation process. However, the addition of tert-butanol had a slight effect on the photodegradation of DCF, which means that the ·OH radicals, formed indirectly, were not the most active species in the process. The pseudo-first-order constant value found in the experiment carried out in ultrapure water was 0.015 min^{-1}, while in the presence of triethanolamine and tert-butanol it was 0.0035 and 0.0073 min^{-1}, respectively. In the experiment under a N_2 bubbling, the concentration of DCF in the solution was steady and no degradation was observed. For that reason, this case could not fit a kinetic equation.

Agreeing with previous reports [18,25], the CB edge of g-C_3N_4 is more negative (−1.19 eV, vs. NHE) than the potential of $O_2/\cdot O_2^-$ (−0.33 eV, vs. NHE) and, therefore, the photoexcited electrons on the CB can reduce the O_2. However, the position of the VB in the exfoliated g-C_3N_4 is not suitable for the direct formation of ·OH, because the potentials of $\cdot OH/OH^-$ (2.38 eV, vs. NHE) and $\cdot OH/H_2O$ (2.72 eV, vs. NHE) are more positive than the VB edge of g-C_3N_4 (1.65 eV, vs. NHE). Nevertheless, the ·OH radical species might be formed from $\cdot O_2^-$ in an indirect manner by the following reduction pathway [24]:

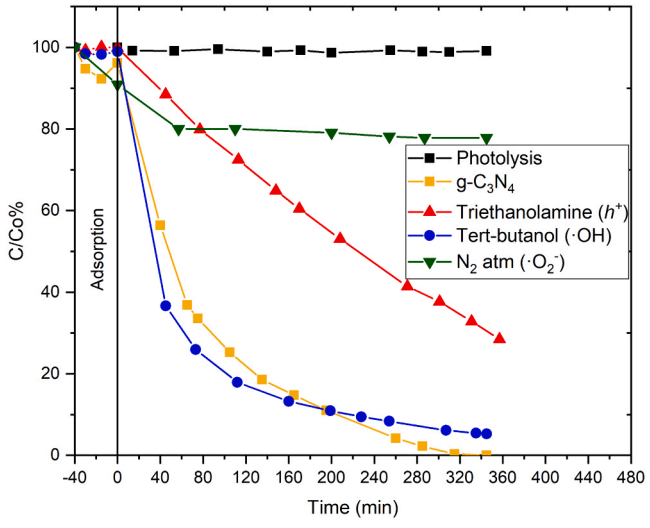

Fig. 3. Effect of different scavengers on the photodegradation of diclofenac with g-C_3N_4 under visible light.

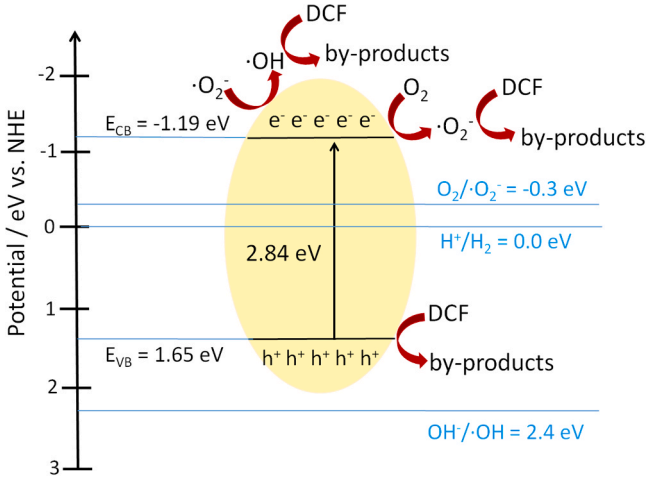

Fig. 4. Schematic diagram of the photoexcited electron-hole separation process for g-C_3N_4 collecting the experimental observations.

Table 1
Summary of UPLC-ESI-MS and MS^2 results for DCF photodegradation with tap water/g-C_3N_4/sunlight.

t_R, min	Experimental mass m/z	Ion	Elementary composition	Error ($\times 10^{-6}$)	Compound formula	MS^2 fragments
1.97 (P1)	242.0807	$[M + H]^+$	$C_{14}H_{12}NO_3^+$	−3.0	$C_{14}H_{11}NO_3$	168.0885 ($C_{12}H_{10}N^+$), 196.0848 ($C_{13}H_{10}NO^+$)
	264.0637	$[M + Na]^+$	$C_{14}H_{11}NO_3Na^+$	1.2		
	240.0658	$[M - H]^-$	$C_{14}H_{10}NO_3^-$	−0.1		
2.29 (P2)	310.0034	$[M + H]^+$	$C_{14}H_{10}NO_3Cl_2^+$	−0.7	$C_{14}H_9NO_3Cl_2$	166.0730 ($C_{12}H_8N^+$), 194.0706 ($C_{13}H_8NO^+$), 201.0442 ($C_{12}H_8NCl^+$), 229.0406 ($C_{13}H_8NOCl^+$), 235.0069 ($C_{12}H_7NCl_2^+$), 264.0109 ($C_{13}H_8NOCl_2^+$), 292.0068 ($C_{14}H_8NO_2Cl_2^+$)
2.42 (P3)	226.0861	$[M + H]^+$	$C_{14}H_{12}NO_2^+$	−1.8	$C_{14}H_{11}NO_2$	180.0893 ($C_{13}H_{10}N^+$)
	224.0716	$[M - H]^-$	$C_{14}H_{10}NO_2^-$	3.1		
2.87 (P4)	260.0466	$[M + H]^+$	$C_{14}H_{11}NO_2Cl^+$	−3.9	$C_{14}H_{10}NO_2Cl$	178.0740 ($C_{13}H_8N^+$) 179.0810 ($C_{13}H_9N^+$) 214.0530 ($C_{13}H_9NCl^+$)
	282.0307	$[M + Na]^+$	$C_{14}H_{10}NO_2ClNa^+$	4.0		
	258.0318	$[M - H]^-$	$C_{14}H_9NO_2Cl^-$	−0.8		
3.38 (DCF)	296.0254	$[M + H]^+$	$C_{14}H_{12}N_2O_2Cl_2^+$	3.7	$C_{14}H_{11}N_2O_2Cl_2$	214.0539 ($C_{13}H_9NCl^+$)
	318.0067	$[M + Na]^+$	$C_{14}H_{11}N_2O_2Cl_2Na^+$	1.3		
	294.0089	$[M - H]^-$	$C_{14}H_{10}N_2O_2Cl_2^-$	0.7		178.0765 ($C_{13}H_{10}N^-$) 214.0563 ($C_{13}H_9NCl^-$)

Table 2
Proposed identification of DCF photodegradation by-products.

Compound formula	Chemical structure proposed	Name	Reported in
$C_{14}H_{11}NO_3$ **P1**	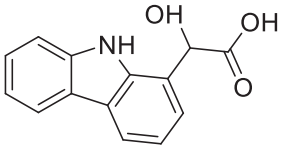	P1a: 2-(9H-carbazol-1-yl)-2-hydroxyacetic acid	
	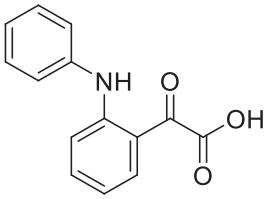	P1b: 2-oxo-2-(2-(phenylamino)phenyl)acetic acid	
$C_{14}H_9NO_3Cl_2$ **P2**	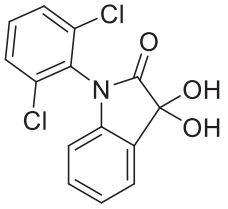	1-(2,6-dichlorophenyl)-3,3-dihydroxyindolin-2-one	
$C_{14}H_{11}NO_2$ **P3**	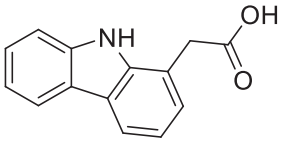	2-(9H-carbazol-1-yl)acetic acid	Koumaki et al. [5], Krakkó et al. [6], Jin et al. [28].
$C_{14}H_{10}NO_2Cl$ **P4**	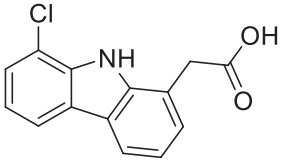	2-(8-chloro-9H-carbazol-1-yl)acetic acid	Koumaki et al. [5], Krakkó et al. [6], Lekkerkerker-Teunissen et al. [7], Zhang et al. [18], Liu et al. [34].
$C_{14}H_{11}N_2O_2Cl_2$ **Diclofenac**	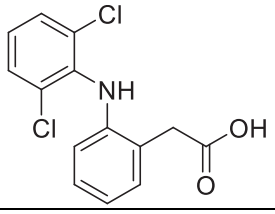	2-(2-((2,6-dichlorophenyl)amino)phenyl)acetic acid	

$$g\text{-}C_3N_4\ (e^-) + O_2 \rightarrow \cdot O_2^-$$

$$g\text{-}C_3N_4\ (e^-) + \cdot O_2^- + 2H^+ \rightarrow H_2O_2$$

$$g\text{-}C_3N_4\ (e^-) + H_2O_2 \rightarrow \cdot OH + OH^-$$

The low efficiency of ·OH scavenging when tert-butanol is added points to a secondary role of this reactive species in the photocatalytic degradation of DCF. However, it seems to be responsible for some of the steps of the DCF degradation (pathway B) proposed and discussed later.

Fig. 4 depicts the schematic diagram of the photoexcited electron-hole separation process for g-C_3N_4, collecting the experimental observations. In summary, based on the results obtained the major reactive species in the photocatalytic oxidation of DCF are the superoxide radicals ($\cdot O_2^-$). In addition, some part of the DCF molecules would be oxidised by the photogenerated holes (h^+) favouring the charge-carrier separation. ·OH radicals formed from superoxide radicals would also support the degradation process.

3.3. Identification of DCF degradation intermediate products

For the identification of DCF by-products, a degraded sample in tap water, irradiated with natural sunlight was analysed by a LC-MS instrument. Fig. S5 depicts a typical chromatogram. It was recorded in positive and negative ESI modes and the absorbance was recorded at 276 nm. Five peaks were detected: 3.38 min (DCF) and four signals at 1.97, 2.29, 2.42 and 2.87 min correspond to DCF photodegradation by-products, hereinafter named as P1, P2, P3 and P4, respectively. Table 1 summarises the main *m/z* signals detected for the chromatographic peaks, the elementary composition with the corresponding mass error, the ions found ($[M+H]^+$, $[M+Na]^+$ and $[M-H]^-$), the MS^2 data of the main ions and the compound formula proposed. Fig. S6 (Supplementary material) contains mass spectra of DCF by-products. The proposed chemical formulas were selected among the plausible possibilities provided by ChemCalc (http://www.chemcalc.org, Institute of Chemistry and Chemical Engineering, Ecole Polytechnique Federale de Lausanne), taking into account the smallest mass error provided as well as the feasibility relating to DCF chemical structure and molecule unsaturation. In all the proposals, mass errors expressed in part per million (ppm) were ≤ 4 ppm.

The first compound (P1) was eluted at 1.97 min with a main signal at *m/z* 242.0807 in the +MS spectrum. It was assigned to the $[M+H]^+$ ion of a DCF intermediate with $C_{14}H_{11}NO_3$ formula and the mass error is −3 ppm. The corresponding signal of the $[M+Na]^+$ ion was also detected at *m/z* 264.0637 with a mass error of 1.2 ppm. Finally, the −MS spectrum shown a main signal at *m/z* 240.0658 assigned to the

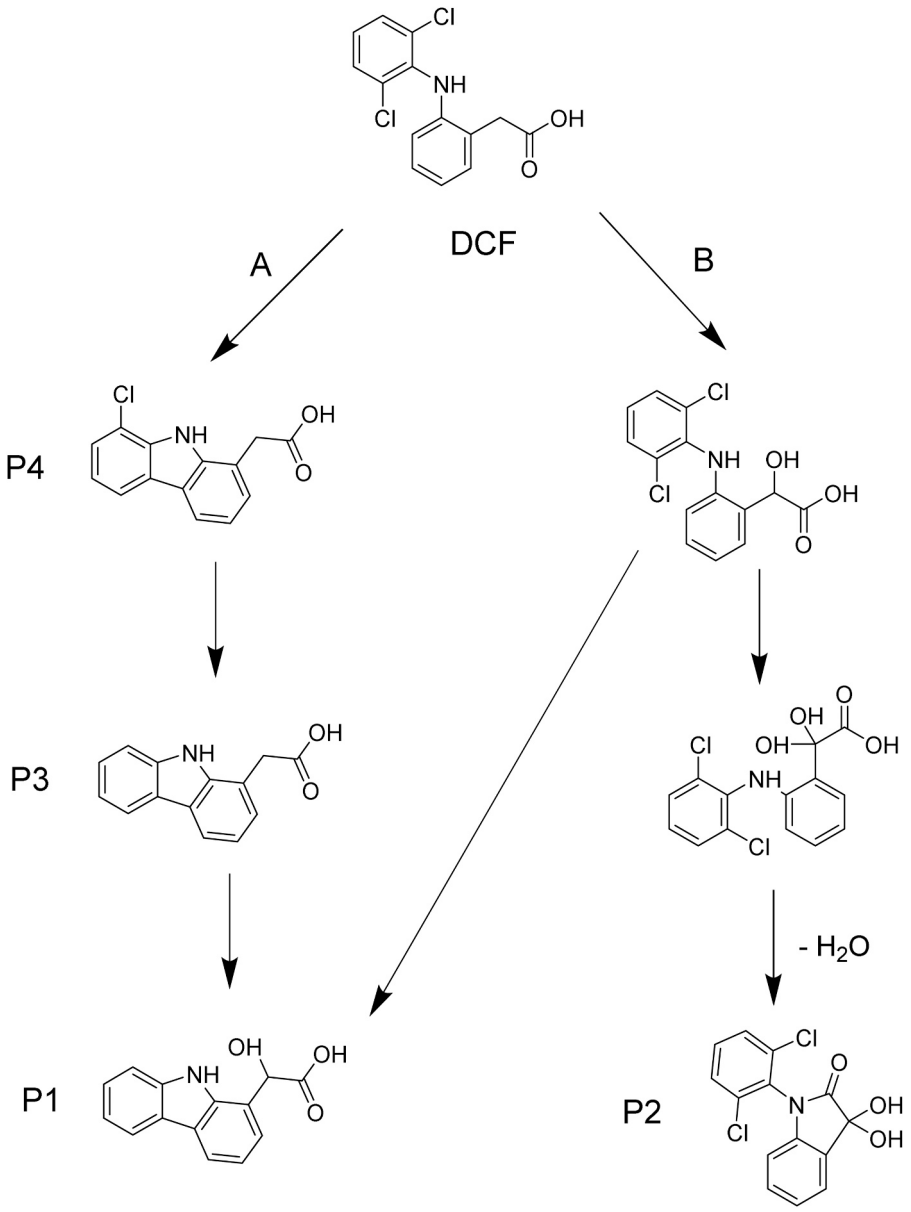

Fig. 5. Possible photodegradation pathway of DCF with g-C_3N_4 nanosheets.

$C_{14}H_{10}NO_3^-$ ion formula with a mass error of −0.1 ppm. Among the possibilities for this by-product with formula $C_{14}H_{11}NO_3$, the proposed structures (Table 2) are: 2-oxo-2-(2-(phenylamino)phenyl)acetic acid (P1b) and 2-(9H-carbazol-1-yl)-2-hydroxyacetic acid (P1a), both can be explain by MS^2 data. The former is more likely based on the structures of the other peaks, because P1a is more likely to be formed from them (Fig. 5). P1a might be formed by the loss of chlorines through superoxide radicals attack, followed by the alpha carbon oxidation. It is consistent with the MS^2 data, as can be seen in Fig. S7 (Supplementary material).

Some authors [5–7] have reported the ion *m/z* 242 in their studies or the ion *m/z* 240 when the negative ionisation mode was used [16]. However, they proposed other structures which are incompatible with our MS^2 data. Three of them proposed a cyclization between the carboxylic acid and the amine group (2-(8-hydroxy-9H-carbazol-1-yl)acetic acid), which cannot be supported by our MS^2 data (Fig. S7 and Table 1) corresponding with the ion formula $C_{12}H_{10}N^+$ and $C_{13}H_{10}NO^+$. On the other hand, Krakkò et al. [6] proposed a structure, which involves a cyclization and breaking the aromatisation of a benzene ring.

The second by-product eluted, P2 (retention time 2.29 min), was the only by-product that was not detected in negative ESI mode. This might suggest that P2 has endured a reaction which involves the carboxylic acid and subsequently does not form anions. It shows a *m/z* signal at 310.0034 that corresponds to the protonated ion of an intermediate product with formula $C_{14}H_9NO_3Cl_2$ (−0.7 ppm mass error). Moreover, the spectrum reveals that the compound should have two chlorine atoms accordingly to its isotopic distribution (*m/z* 310 and 312 being the latter around 60% of the former). Considering the chemical structure of DCF, the by-product proposed is 1-(2,6-dichlorophenyl)-3,3-dihydroxyindolin-2-one, which corresponds to the oxidation of the alpha carbon (due to the attack of ·OH or the action of $\cdot O_2^-$) and the cycling reaction between the carboxylic acid and the amine group. Other authors [11,28,34] also found the *m/z* 310, although they proposed different structures which are incompatible with our MS^2 data. Jin et al. [28] found the same MS^2 fragment (*m/z* 201) that we found, which seems to be an ion which has lost the three oxygen atoms ($C_{12}H_8NCl^+$) that its precursor had. However, for the structure they proposed [28] ((E)-2-(6-((2,6-dichlorophenyl)imino)-3-oxocyclohexa-1,4-dien-1-yl)acetic acid) this is fairly unlikely to happen. Furthermore, it is a plausible alternative that the

real by-product formed in the photodegradation process was the compound 2-(2-((2,6-dichlorophenyl)amino)phenyl)-2,2-dihydroxyacetic acid ($C_{14}H_{11}Cl_2NO_4$), which could suffer dehydration by losing a H_2O molecule in the ionisation source; hence we detected the *m/z* 310.

A third chromatographic peak was eluted at 2.42 min (P3). The *m/z* signal at 226.0861 corresponds to a protonated by-product whose formula is $C_{14}H_{11}NO_2$ with a mass error of −1.8 ppm. The corresponding anion was also detected in the negative ESI at *m/z* 224.0716 (3.1 ppm mass error). This compound has been reported previously in the literature using the same catalyst and a photochemical reactor simulating visible light. Other authors found it in photolysis experiments [5,6,28]. In all cases, the authors proposed the same structure as we did in the present study: 2-(9H-carbazol-1-yl)acetic acid. The main signal in the MS^2 positive spectrum at *m/z* 180.0893 corresponding to the decarboxylation of the by-product with ion molecular formula $C_{13}H_{10}N^+$.

The last by-product (P4) was detected at 2.87 min and showed two main *m/z* signals. One at *m/z* 260.0466 in positive ESI that was assigned to the protonated degradation product with formula $C_{14}H_{10}NO_2Cl$ and another at *m/z* 282.0307, assigned to the sodiated product, with mass errors of −3.9 and 4 ppm respectively. In the negative ESI, the respective deprotonated anion was also detected at *m/z* 258.0318 (−0.8 ppm mass error). The compound proposed in the present study, 2-(8-chloro-9H-carbazol-1-yl) acetic acid, has been reported by other authors [5–7,18,34]. This compound is supported by the MS^2 data (Table 1 and Fig. S7), with a signal at *m/z* 214.0530 assigned to the ion formula $C_{13}H_9NCl^+$, a decarboxylation of its precursor. Both compounds P4 and P3 arise from successive dechlorinations of DCF and cyclization provoked by the superoxide radical attack as observed in the photocatalytic degradation of chlorophenol derivatives [35].

The last chromatographic peak at 3.38 min corresponded to DCF. It was detected in UV, +MS and −MS chromatograms. The protonated DCF ion at *m/z* 296.0254 (3.7 ppm mass error), the sodiated ion and the deprotonated ion were identified. The proposed structures for the MS^2 fragment ions are summarised in Fig. S7.

Finally, it must be mentioned that all by-products and the diclofenac itself have been classified according to Cramer rules as high toxicity hazards (class III).

3.4. Degradation mechanism and pathway

According to the previous results, there seem to be two main degradation routes (Fig. 5). One of them involves the loss of chlorine groups (pathway A), whereas pathway B seems to be favoured more by the oxidation of the alpha carbon. Moreover, P1 might be formed following both pathways. The by-products P1 and P3 were detected in the photolysis studies with natural sunlight and the pathway A by-products have been mainly described on the literature in photolysis studies [5–7]. This suggests that pathway A could be ascribed to the influence of the irradiation, although the superoxide radicals' dechlorination ability would also be responsible for this pathway to some extent, as observed in the LED light experiments for which photolysis can be ruled out.

The formation of by-products in pathway B may be influenced more by the action of the catalyst and the attack of ·OH (or the action of the superoxide radicals), although P1 could be formed by both routes.

On the other hand, the kinetics of the by-products are shown in Fig. S8. The by-product P3 seems to be the main degradation product. The four by-products were totally degraded except in the experiment with tap water and LEDs radiation, where P3 and P4 persist in the solution after 480 min of irradiation. Furthermore, the four by-products were only found in the experiments with natural sunlight, whereas in the experiments with LED light and ultrapure water, P4 was not detected and in the experiment with tap water and LED light, P3 and P4 were the only by-products observed. In the experiments with natural sunlight the depletion of DCF was faster and the four by-products were formed and degraded in less than 100 min due to the power of the irradiation.

4. Conclusions

The usefulness of g-C_3N_4 nanosheets to photodegrade DCF with different sources of irradiation (high energy and low energy) has been confirmed. The photodegradations of DCF exhibited higher degradation rates in tap water than in ultrapure water. Also, when the diclofenac solution was irradiated with natural sunlight it exhibited higher degradation rates than with the low power visible LED lights. The fastest degradation took place in tap water with natural sunlight, where the pseudo-first-order kinetic constant was 0.383 min^{-1}. The tentative identification of the four by-products was performed by high-resolution mass spectrometry (with mass errors < 4 ppm) to determine their elemental composition. The debates on the MS^2 data were of the utmost importance in order to check the plausible chemical structures proposed and discard some of them, which was one of the novel aspects of this study. Two tentative structures for the four intermediate products have been reported for the first time: 1-(2,6-dichlorophenyl)-3,3-dihydroxyindolin-2-one and 2-(9H-carbazol-1-yl)-2-hydroxyacetic acid. Bearing in mind the degraded products detected, the photodegradation of DCF seems mostly to be caused by two routes: the loss of chlorine groups and the oxidation of the alpha carbon. Furthermore, the main active species involved in the photocatalytic process were the superoxide radicals, producing the dechlorination of DCF, and the photogenerated holes in the valence band of the g-C_3N_4, which favours the DCF oxidation process.

CRediT authorship contribution statement

Marta Jiménez-Salcedo: Investigation, Visualization, Writing - original draft. **Miguel Monge:** Project administration, Funding acquisition, Conceptualization, Supervision, Writing - review & editing (Catalyst synthesis and characterisation). **María Teresa Tena:** Conceptualization, Supervision, Writing - review & editing (Mass spectrometry and kinetics).

Declaration of Competing Interest

The authors declare that they have no known competing financial interests or personal relationships that could have appeared to influence the work reported in this paper.

Acknowledgements

We thank the D.G.I. MINECO/FEDER (project number PID2019-104379RB-C22 (AEI/FEDER, UE)) and the EC support through the FEDER Project NUTRIA (EFA 356/19) for financial support. We also thank the University of La Rioja for M.J.-S.'s predoctoral grant.

Appendix A. Supplementary material

Supplementary data associated with this article can be found in the online version at doi:10.1016/j.jece.2021.105827.

References

[1] T. Aus der Beek, F.A. Weber, A. Bergmann, S. Hickmann, I. Ebert, A. Hein, A. Küster, Pharmaceuticals in the environment—global occurrences and perspectives, Environ. Toxicol. Chem. 35 (2016) 823–835.
[2] M. Patel, R. Kumar, K. Kishor, T. Mlsna, C.U. Pittman Jr., D. Mohan, Pharmaceuticals of emerging concern in aquatic systems: chemistry, occurrence, effects, and removal methods, Chem. Rev. 119 (2019) 3510–3673.
[3] P. Chen, Q. Zhang, L. Shen, R. Li, C. Tan, T. Chen, H. Liu, Y. Liu, Z. Cai, G. Liu, W. Lv, Insights into the synergetic mechanism of a combined vis-RGO/TiO_2/peroxodisulfate system for the degradation of PPCPs: kinetics, environmental factors and products, Chemosphere 216 (2019) 341–351.
[4] J. Nieto-Sandoval, M. Munoz, Z.M. de Pedro, J.A. Casas, Catalytic hydrodechlorination as polishing step in drinking water treatment for the removal of chlorinated micropollutants, Sep. Purif. Technol. 227 (2019), 115717.

[5] E. Koumaki, D. Mamais, C. Noutsopoulos, M.C. Nika, A.A. Bletsou, N.S. Thomaidis, A. Eftaxias, G. Stratogianni, Degradation of emerging contaminants from water under natural sunlight: the effect of season, pH, humic acids and nitrate and identification of photodegradation by-products, Chemosphere 138 (2015) 675–681.
[6] D. Krakkò, E. Gombos, V. Licul-Kucera, S. Dobe, V.G. Mihucz, G. Zaray, Enhanced photolytic and photooxidative treatments for removal of selected pharmaceutical ingredients and their degradation products in water matrices, Microchem. J. 150 (2019), 104136.
[7] K. Lekkerkerker-Teunissen, M.J. Benotti, S.A. Snyder, H.C. van Dijk, Transformation of atrazine, carbamazepine, diclofenac and sulfamethoxazole by low and medium pressure UV and UV/H_2O_2 treatment, Sep. Purif. Technol. 96 (2012) 33–43.
[8] J. Madhavan, P.S.S. Kumar, S. Anandan, M. Zhou, F. Grieser, M. Ashokkumar, Ultrasound assisted photocatalytic degradation of diclofenaco in an aqueous environment, Chemosphere 80 (2010) 747–752.
[9] D. Meroni, M. Jimenez-Salcedo, E. Falletta, B.M. Bresolinc, C.F. Kaitd, D. C. Boffitoe, C.L. Bianchia, C. Pirola, Sonophotocatalytic degradation of sodium diclofenac using low power ultrasound and micro sized TiO_2, Ultrason. Sonochem. 67 (2020), 105123.
[10] A. Smýkalová, B. Sokolová, K. Foniok, V. Matejka, P. Praus, Photocatalytic degradation of selected pharmaceuticals using g-C_3N_4 and TiO_2 nanomaterials, Nanomaterials 9 (2019) 1194 (Basel, Switzerland).
[11] F. Liu, J. Liang, L. Chen, M. Tong, W. Liu, Photocatalytic removal of diclofenac by Ti doped BiOI microspheres under visible light irradiation: kinetics, mechanism, and pathways, J. Mol. Liq. 275 (2019) 807–814.
[12] N.F.F. Moreira, M.J. Sampaio, A.R. Ribeiro, C.G. Silva, J.L. Faria, A.M.T. Silva, Metal-free g-C_3N_4 photocatalysis of organic micropollutants in urban wastewater under visible light, Appl. Catal. B 248 (2019) 184–192.
[13] A.N. Oliveros, J.A.I. Pimentel, M.D.G. de Luna, S. Garcia-Segurac, R.R.M. Abarca, R.A. Doong, Visible-light photocatalytic diclofenac removal by tunable vanadium pentoxide/boron-doped graphitic carbon nitride composite, Chem. Eng. J. 403 (2021), 126213.
[14] H. Shao, X. Zhao, Y. Wang, R. Mao, Y. Wang, M. Qiao, S. Zhao, Y. Zhu, Synergetic activation of peroxymonosulfate by Co_3O_4modified g-C_3N_4 for enhanced degradation of diclofenac sodium under visible lightirradiation, Appl. Catal. B 218 (2017) 810–818.
[15] Z. Hu, X. Cai, Z. Wang, S. Li, Z. Wang, X. Xie, Construction of carbon-doped supramolecule-based g-C_3N_4/TiO_2 composites for removal of diclofenac and carbamazepine: a comparative study of operating parameters, mechanisms, degradation pathways, J. Hazard. Mater. 380 (2019), 120812.
[16] J. He, J. Yang, F. Jiang, P. Liu, M. Zhu, Photo-assisted peroxymonosulfate activation via 2D/2D, Chemosphere 258 (2020), 127339.
[17] W. Zhang, L. Zhou, H. Deng, Ag modified g-C_3N_4 composites with enhanced visible-lightphotocatalytic activity for diclofenac degradation, J. Mol. Catal. A Chem. 423 (2016) 270–276.
[18] W. Zhang, L. Zhou, J. Shi, H. Deng, Fabrication of novel visible-light-driven AgI/g-C_3N_4 composites with enhanced visible-light photocatalytic activity for diclofenac degradation, J. Colloid Interface Sci. 496 (2017) 167–176.
[19] W. Zhang, L. Zhou, J. Shi, H. Deng, Synthesis of Ag_3PO_4/g-C_3N_4 composite with enhanced photocatalytic performance for the photodegradation of diclofenac under visible light irradiation, Catalysts 8 (2018) 45.
[20] W.J. Ong, L.L. Tan, Y.H. Ng, S.T. Yong, S.P. Chai, Graphitic carbon nitride (g-C_3N_4)-based photocatalysts for artificial photosynthesis and environmental remediation: are we a step closer to achieving sustainability? Chem. Rev. 116 (2016) 7159–7329.
[21] M. Jiménez-Salcedo, M. Monge, M.T. Tena, Photocatalytic degradation of ibuprofen in water using TiO_2/UV and g-C_3N_4/visible light: study of intermediate degradation products by liquid chromatography coupled to high-resolution mass spectrometry, Chemosphere 215 (2019) 605–618.
[22] M. Jiménez-Salcedo, M. Monge, M.T. Tena, Study of intermediate by-products and mechanism of the photocatalytic degradation of ciprofloxacin in water using graphitized carbon nitride nanosheets, Chemosphere 247 (2020), 125910.
[23] S.C. Yan, Z.S. Li, Z.G. Zou, Photodegradation performance of g-C_3N_4 fabricated by directly heating melamine, Langmuir 25 (2009) 10397–10401.
[24] S.P. Pattnaik, A. Behera, S. Martha, R. Acharya, K. Parida, Facile synthesis of exfoliated graphitic carbon nitride for photocatalytic degradation of ciprofloxacin under solar irradiation, J. Mater. Sci. 54 (2019) 5726–5742.
[25] S. Chen, Y. Hu, S. Meng, X. Fu, Study on the separation mechanisms of photogenerated electrons and holes for composite photocatalyst g-C_3N_4-WO_3, Appl. Catal. B 150–151 (2014) 564–573.
[26] A. Thomas, A. Fischer, F. Goettmann, M. Antonietti, J.-O. Müller, R. Schlögl, J. M. Carlsson, Graphitic carbon nitride materials: variation of structure and morphology and their use as metal-free catalysts, J. Mater. Chem. 18 (2008) 4893–4908.
[27] F. Fina, H. Ménard, J.T.S. Irvine, The effect of Pt NPs crystallinity and distribution on the photocatalytic activity of Pt–g-C_3N_4, Phys. Chem. Chem. Phys. 17 (2015) 13929–13936.
[28] X. Jin, Y. Wu, Q. Zhang, F. Wang, P. Chen, H. Liu, S. Huang, J. Wu, N. Tu, W. Lv, G. Liu, Defect-modified reduced graphitic carbon nitride (RCN) enhanced oxidation performance for photocatalytic degradation of diclofenac, Chemosphere 258 (2020), 127343.
[29] P. Iovino, S. Chianese, S. Canzano, M. Prisciandaro, D. Musmarra, Ibuprofen photodegradation in aqueous solutions, Environ. Sci. Pollut. Res. 23 (2016) 22993–23004.
[30] Z. Yang, J. Yan, J. Lian, H. Xu, X. She, H. Li, *g*-C_3N_4/TiO_2 nanocomposites for degradation of ciprofloxacin under visible light irradiation, ChemistrySelect 1 (2016) 5679–5685.
[31] H. Wang, J. Li, C. Ma, Q. Guan, Z. Lu, P. Huo, Y. Yan, Melamine modified P25 with heating method and enhanced the photocatalytic activity on degradation of ciprofloxacin, Appl. Surf. Sci. 329 (2015) 17–22.
[32] R. Hao, G. Wang, H. Tang, L. Sun, C. Xu, D. Han, Template-free preparation of macro/mesoporous g-C_3N_4/TiO_2 heterojuction photocatalysts with enhanced visible light photocatalytic activity, Appl. Catal. B 187 (2016) 47–58.
[33] N. Lu, P. Wang, Y. Su, H. Yu, N. Liu, X. Quan, Construction of Z-scheme *g*-C_3N_4/RGO/WO_3 with in situ photoreduced graphene oxide as electron mediator for efficient photocatalytic degradation of ciprofloxacin, Chemosphere 215 (2019) 444–453.
[34] W. Liu, Y. Li, F. Liu, W. Jiang, D. Zhang, J. Liang, Visible-light-driven photocatalytic degradation of diclofenac by carbon quantum dots modified porous g-C_3N_4: mechanisms, degradation pathway and DFT calculation, Water Res. 151 (2019) 8–19.
[35] Y. Li, J. Niu, L. Yin, W. Wang, Y. Bao, J. Chen, Y. Duan, Photocatalytic degradation kinetics and mechanism of pentachlorophenol based on superoxide radicals, J. Environ. Sci. 23 (2011) 1911–1918.